

Domain formation due to surface steps in topological insulator Bi₂Te₃ thin films grown on Si (111) by molecular beam epitaxy

S. Borisova, J. Kampmeier, M. Luysberg, G. Mussler, and D. Grützmacher

Citation: [Applied Physics Letters](#) **103**, 081902 (2013); doi: 10.1063/1.4818456

View online: <http://dx.doi.org/10.1063/1.4818456>

View Table of Contents: <http://scitation.aip.org/content/aip/journal/apl/103/8?ver=pdfcov>

Published by the [AIP Publishing](#)

Articles you may be interested in

[Electronic structure and morphology of epitaxial Bi₂Te₂Se topological insulator films](#)

J. Appl. Phys. **116**, 193708 (2014); 10.1063/1.4902010

[Two-dimensional weak anti-localization in Bi₂Te₃ thin film grown on Si\(111\)-\(7×7\) surface by molecular beam epitaxy](#)

Appl. Phys. Lett. **102**, 163118 (2013); 10.1063/1.4803018

[Molecular beam epitaxy of bilayer Bi\(111\) films on topological insulator Bi₂Te₃: A scanning tunneling microscopy study](#)

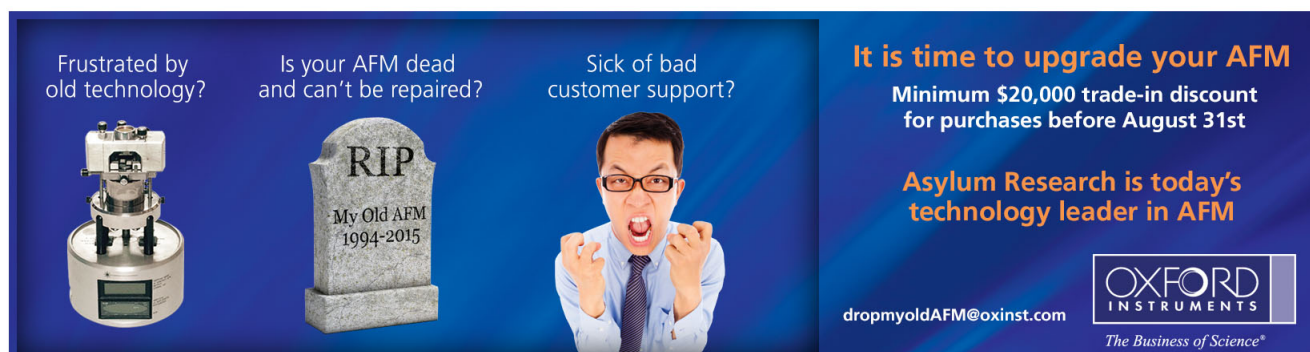
Appl. Phys. Lett. **101**, 081603 (2012); 10.1063/1.4747715

[Robust surface electronic properties of topological insulators: Bi₂Te₃ films grown by molecular beam epitaxy](#)

Appl. Phys. Lett. **98**, 222503 (2011); 10.1063/1.3595309

[Epitaxial growth of Bi₂Se₃ topological insulator thin films on Si \(111\)](#)

J. Appl. Phys. **109**, 103702 (2011); 10.1063/1.3585673

An advertisement for Asylum Research. It features a blue background with three panels. The first panel shows a white AFM head on a base with the text 'Frustrated by old technology?'. The second panel shows a tombstone with 'RIP' and 'My Old AFM 1994-2015' with the text 'Is your AFM dead and can't be repaired?'. The third panel shows a man with glasses and a tie, looking frustrated with his hands raised, with the text 'Sick of bad customer support?'. To the right, a large white box contains the text 'It is time to upgrade your AFM', 'Minimum \$20,000 trade-in discount for purchases before August 31st', and 'Asylum Research is today's technology leader in AFM'. At the bottom right is the Oxford Instruments logo with the tagline 'The Business of Science®' and the email 'dropmyoldAFM@oxinst.com'.

Domain formation due to surface steps in topological insulator Bi_2Te_3 thin films grown on Si (111) by molecular beam epitaxy

S. Borisova,^{1,2} J. Kampmeier,^{1,2} M. Luysberg,³ G. Mussler,^{1,2} and D. Grützmacher^{1,2}

¹Peter Grünberg Institute-9, Forschungszentrum Jülich, Jülich 52425, Germany

²Jülich Aachen Research Alliance, Fundamentals of Future Information Technologies, Jülich 52425, Germany

³Peter Grünberg Institute-5 and Ernst Ruska-Centre for Microscopy and Spectroscopy with Electrons, Forschungszentrum Jülich, Jülich 52425, Germany

(Received 24 April 2013; accepted 26 July 2013; published online 19 August 2013)

The atomic structure of topological insulators Bi_2Te_3 thin films on Si (111) substrates grown in van der Waals mode by molecular beam epitaxy has been investigated by *in situ* scanning tunneling microscopy and scanning transmission electron microscopy. Besides single and multiple quintuple layer (QL) steps, which are typical for the step-flow mode of growth, a number of 0.4 QL steps is observed. We determine that these steps originate from single steps at the substrate surface causing domain boundaries in the Bi_2Te_3 film. Due to the peculiar structure of these domain boundaries the domains are stable and penetrate throughout the entire film. © 2013 AIP Publishing LLC. [<http://dx.doi.org/10.1063/1.4818456>]

Complex hexagonal layered materials such as Bi_2Te_3 , Bi_2Se_3 , Sb_2Te_3 and their alloys have recently attracted attention due to their outstanding properties as topological insulators (TIs).¹ Insulating in bulk, these materials possess metallic surface states located within the bulk band gap and protected against elastic backscattering at nonmagnetic impurities by time-reversal symmetry.² Exciting a great interest to theoretical studies, these materials present significant challenges to the experimental observation of this feature due to the unintentional bulk doping.^{3,4} Indeed, the crystal structure of 3D TIs is prone to a high density of anti-site defects, causing a shift of Fermi energy within the whole band gap and beyond.⁵ This circumstance may be overcome using high quality ultrathin films in order to exclude the contribution of the bulk charge carriers or by means of counter-doping.⁶ Providing accurate control under the film thicknesses and the doping level, the MBE technique offers routes in order to overcome this problem. Recently, growth of perfect TI single crystalline films by MBE has been demonstrated on various substrates both highly mismatched, such as graphene,⁷ Si,^{8,9} GaAs,¹⁰ and nearly lattice matched, for example, InP¹¹ or BaF_2 .⁶ Thus, the lattice mismatch between the film and substrate is not a crucial parameter, since the growth takes place in the van der Waals growth mode.^{12,13} Furthermore, the grown films are only weakly bound to the substrate and, therefore, fully relaxed. Thus, the quality of the films is not significantly influenced by strain due to the lattice mismatch, in contrast to the conventional heteroepitaxy. Besides strain-induced defects, epitaxial growth on substrates with different crystal structure may also cause the formation of antiphase domains due to the substrate steps, for example in GaAs on Si.^{14–16} Therefore, one could assume the presence of domain boundaries in 3D TI films, affecting their electrical properties. However, both any corresponding calculations and experimental information are missing so far.

Bi_2Te_3 possesses a complicated crystal structure with a unit cell built from three so-called quintuple layers (QLs). Every QL consists of five alternating and strongly bound

Bi and Te atomic sheets in the following sequence in the [0001] direction: Te I-Bi-Te II-Bi-Te I. The coupling between the QLs is weak due to its van der Waals nature and allows layer-by-layer growth in the step-flow mode with a QL as a unit.^{17–19} The substrate determines the crystallographic z axis of the Bi_2Te_3 film perpendicular to the substrate surface. The orientation of the film matches with the Si substrate orientation.⁸ Despite the lattice mismatch of 14%, the film is fully relaxed even within the 1st QL.¹⁷ Generally, the growth on Si (111) can be separated in three phases consisting of the substrate passivation by Te, the 3D island growth, and the subsequent 2D QL step-flow mode growth of Bi_2Te_3 films without formation of any amorphous buffer layer.¹⁶ The crystal structure of Bi_2Te_3 allows the presence of two energetically equivalent twin domains. Indeed, TEM observations reveal both, vertical and horizontal domain boundaries.^{17,20,21} One of the twin domains can be locally overgrown by the other domain at the thickness of several nm and does not cause any threading or planar defects, observable at the film surface. Previously, it has been reported on a number of sub QL steps which can neither be attributed to the single unit steps usually found in the step-flow mode nor to the twin domains. However, the high dislocation density has not allowed us to determine the origin of these steps so far.¹⁷ The sub QL steps have been observed in Bi_2Se_3 films grown on Bi-covered Si (111), however, these steps disappear with increasing film thickness and their atomic structure have not been investigated.²² In this letter, we report on the atomic structure of domains due to single steps on the substrate surface, observed in topological insulator Bi_2Te_3 thin film on Si (111) grown in the van der Waals epitaxy mode by MBE. These domains are studied by *in situ* scanning tunneling microscopy (STM) and high-resolution transmission electron microscopy (HR STEM).

The MBE growth of Bi_2Te_3 films were realized in an ultra-high vacuum (UHV) chamber (base pressure 2×10^{-9} mbar) equipped with standard effusion cells for Bi and Te. Prior to the deposition, n-doped Si (111) substrates ($3.6\text{--}5.5\ \Omega\text{cm}$) have been chemically cleaned in piranha

solution (H_2SO_4 2:1 H_2O_2) and in 1% hydrofluoric acid. The clean Si surface is thereby passivated by a monolayer of hydrogen. After immediate transfer to the UHV MBE a pre-growth annealing has been performed in two different ways for different samples: for the so-called low temperature annealing the substrates were heated up to 700°C for 20 min, in order to desorb the H passivation layer. Alternatively, the high temperature annealing has been carried out for 30 min at 960°C . The subsequent slow cool down to 700°C ($\sim 1^\circ\text{C/s}$) provides an atomically flat surface with a low roughness and density of surface defects as well as a stable (7×7) reconstruction, confirmed by RHEED. Atomic Bi and Te have been evaporated at the source temperatures of $T_{\text{Bi}} = 470^\circ\text{C}$, $T_{\text{Te}} = 380^\circ\text{C}$. The growth took place under Te overpressure at $T_{\text{sub}} = 300^\circ\text{C}$, providing a high quality single crystalline Bi_2Te_3 film.⁸ The growth rate was 4 nm/h. Directly after Bi_2Te_3 deposition, the samples have been transferred to the *in situ* STM chamber under UHV conditions. The STM measurements have been performed at room temperature. Additionally, the Bi_2Te_3 films have been investigated *ex situ* by atomic force microscopy (AFM) and by HR STEM using an aberration corrected STEM (FEI Titan 80–300). Cross-sectional specimens were prepared by conventional grinding techniques and final ion milling with Ar ions.

Ex situ AFM measurements of 11 nm thick Bi_2Te_3 films show islands with diameters of 2–3 μm featuring large atomically flat areas in between (see Figure 1(a)). The islands possess flat terraces with a constant width of nearly 300 nm separated by the single QL steps. This morphology of the film confirms the step-flow mode of growth with a QL as the growth unit. It is remarkable that every terrace replicates the shape of the previous one. Therefore, we assume that the lateral growth is accompanied by the vertical growth of the pyramids, due to the limited surface diffusion length of the adatoms. Indeed, at the moment when the width of the topmost terrace becomes larger than twice the diffusion length, a new terrace starts to nucleate on top of it. Mainly, this growth model has been used so far, in order to describe the growth of Bi_2Te_3 and related materials by thin film deposition techniques. However, a closer look at the surface

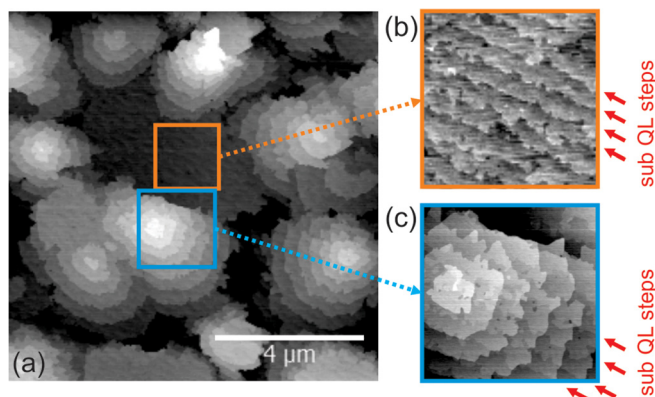


FIG. 1. (a) Large scale AFM image of 11 nm thick Bi_2Te_3 film. Flat terraces are separated by single QL steps exhibiting the step-flow mode of growth. Besides the single QL steps, a regular pattern of sub QL steps is observed in the flat area (b) as well as in the pyramids (c). These steps proceed along a certain direction through the entire substrate and maintain undisturbed when crossing the pyramids.

topography shows a regular pattern of shallow parallel steps (see Figure 1(b)). The distance between the steps is approximately 100 nm. The steps propagate over the whole substrate along a certain direction. Figure 1(c) shows the step pattern to maintain undisturbed while the steps intersect the pyramids.

In situ STM investigations of the surface topography have been performed under UHV conditions in order to investigate the morphology of these steps directly after deposition without exposing the surface to the ambient atmosphere. In accordance to the AFM data, the STM image in Figure 2(a) shows the presence of concentric single QL steps intersected by a regular pattern of nearly parallel sub-QL steps (indicated by red arrows). The height of the sub-QL steps has a constant value of 0.4 nm (see the height profile in Figure 2(b)). This value is within the inaccuracy of the measurement, compared to the calculated height of a Te I–Bi step of 0.371 nm.²³ Since such a step consist of two atomic sheets (compared to 5 atomic sheets building a single QL), we will further call it as a 0.4 QL step. The orange arrow in Figure 2(a) points to the intersection of a single QL step and a 0.4 QL step. The 0.4 QL step propagates through the neighboring single QL terraces, i.e., the step-flow growth occurs independently and the 0.4 QL steps appear to have no significant impact on the step flow mode of growth. Since the growth of topological insulators and the morphology of the films is strongly influenced by a number of parameters (substrate material, surface preparation before the growth, substrate temperature, growth rates), we have compared this film to a film grown on a high temperature annealed substrate using the same recipe (see Figure 2(c)). Again, a set of 0.4 QL steps as well as single QL steps have been observed (see Figure 2(d)). Although the spacing between the single

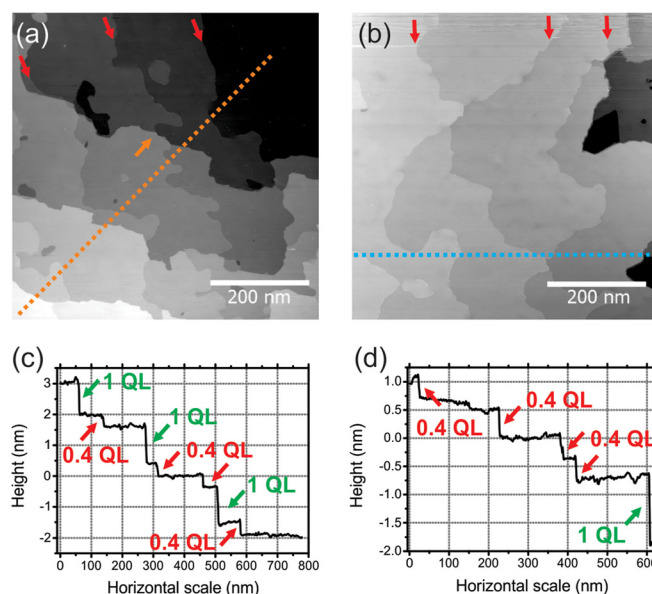


FIG. 2. *In situ* STM images depicting the surface morphology of 11 nm thick Bi_2Te_3 films grown on Si (111) substrates (a) overgrown after H-desorption at 700°C , (b) *in situ* annealed at 960°C in order to obtain (7×7) reconstruction. (c), (d) The corresponding height profiles reveal the presence of a number of sub QL steps between the single QL steps, typically of 0.4 QL in height. The intersection of a QL step and a 0.4 QL step (indicated by the orange arrow in (a)) demonstrates that these sub QL steps are not disturbed by the step-flow mode of growth.

QL steps is significantly increased compared to the low-temperature annealed substrate, the width of 0.4 QL steps is in average unchanged.

The observed morphology of the sub QL steps let us assume that the sub QL steps may originate at the substrate surface. In order to prove this assumption, the films have been studied by STM at the early nucleation stage of growth after deposition of nominally 1 nm Bi_2Te_3 . The atomically flat single crystalline islands have been observed at the low temperature annealed substrate (see Figure 3(a)). Due to their small size and the high density of the islands, no sub QL steps can be recognized. However, different terraces between the islands are seen. To guide the eye, colored labels are placed between the islands in the areas of the same height. The legend to the labels is shown in Figure 3(b). The labels point out the presence of 0.4 QL height difference between the neighboring terraces. Moreover, the average size of the terraces has been determined as the distance between the dotted lines in Figure 3(a), separating the areas with the predominant amounts of the certain terraces. Identically to the films of 11 nm thickness, the step pattern is regular, the terrace edges are parallel and the width of the terraces is about 100 nm. Thus, the observed 0.4 QL steps replicate the substrate steps propagating throughout the entire film. The width of the Bi_2Te_3 terraces is in accordance to the distance between single steps in the Si substrate with nominally no miscut. Due to the lower density of surface defects, the surface diffusion length of the adatoms is significantly higher in case of the high temperature annealed substrate. Therefore, the nominally 1 nm thick film grown on the high temperature annealed substrate exhibits a low density of islands. At the same time, the 0.4 QL steps are still present at the surface (see Figure 3(c)). Thus, these steps should be attributed to

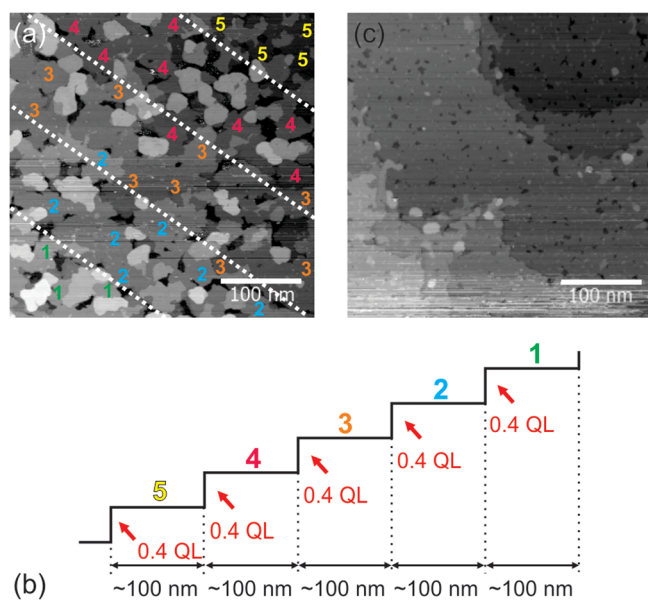


FIG. 3. (a) *In situ* STM image depicting the surface morphology of 1 nm thick Bi_2Te_3 on Si (111) substrate, overgrown after H-desorption at 700 °C. The terraces are indicated by numbers from 1 to 5 for convenience (b). A regular pattern of atomically flat terraces with the width of 100–150 nm separated by 0.4 nm steps is observed. (c) Surface morphology of 1 nm thick Bi_2Te_3 on Si (111) substrate, *in situ* annealed at 960 °C. Terraces separated by 0.4 nm steps are revealed. The terraces are atomically flat and possess a small number of holes and islands compared to (a).

the substrate morphology rather than to any peculiarities of the crystal structure or growth dynamics of Bi_2Te_3 .

These findings have been confirmed utilizing high resolution cross sectional HR STEM. An atomically resolved image of the Bi_2Te_3 film close to the single step on a Si substrate is presented in Figure 4(a). The image displays a domain boundary, originating exactly at the substrate step and proceeding throughout the entire film. The domains at the boundary have a remarkable atomic structure: two domains are vertically shifted relative to each other by two atomic sheets (i.e., 0.4 QL). Figure 4(b) depicts the correspondent atomic model. Here, the vertical stacking sequence (ABCABC...) maintains undisturbed. Moreover, three of five atomic sheets match each other, whereas two of them change from Bi to Te and vice versa over the domain boundary (indicated by red triangles). Since the van der Waals gap between the QLs is vertically shifted by 0.4 QL, a 0.4 QL is present at the film surface. Therefore, the STEM data is in good agreement with the conclusions based on the previously presented STM investigation.

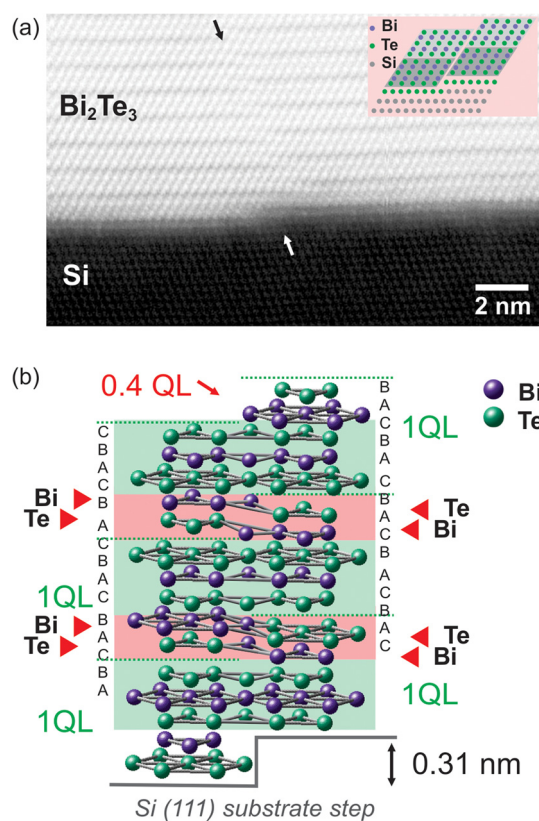


FIG. 4. (a) Cross-section of a Bi_2Te_3 film on Si (111) by HR STEM in (110) projection of Si. The HR STEM image indicates a domain boundary, originating at a single substrate steps. The domain boundary propagates through the complete film and causes a 0.4 QL step on the surface. The inset shows the corresponding atomic model. The stacking sequence (A, B, C) of the atomic sheets remains completely undisturbed at the domain boundary. This is indicated by diagonal lines (atom rows) continuing over the boundary. (b) The crystal model explains the atomic structure of the domain boundary: three of the atomic layers of each QL (marked by green background) penetrate almost undisturbed through the domain boundary, whereas two of the atomic layers of each QL (marked by red background) change from Bi to Te and vice versa (depicted by red triangles). The QLs are indicated by dotted green lines. The stacking sequence (A, B, C) of the atomic sheets remains completely undisturbed at the domain boundary.

In principle, these domains are similar to the antiphase domains originating at the single substrate steps, for the materials grown on substrates with the different crystal structure (particularly, lattice constants in the growth direction). The classical example is the growth of GaAs on Si.^{14–16} Due to the complicated structure of Bi₂Te₃, the domain structure is different though. Single steps on Si (111) are of 0.31 nm in height. The step height of 0.4 QL in Bi₂Te₃ has the best match to these steps on Si. The observed domains are stable and the density of the domain boundaries is equal to the density of the single substrate steps. Thus, this mechanism is preferable compared to the effects provided by the weak van der Waals bonding, i.e., the easy bending of the QLs and the capability of the islands to migrate in the beginning of growth.¹⁷

In summary, our study presents domains in Bi₂Te₃ on Si (111), which appear due to the single steps on the Si substrate surface. The domain boundaries cause a regular pattern of parallel 0.4 QL steps observed on the surface. Combining the STM and STEM data, we ascertain that the QLs of the neighboring domains are vertically shifted by 0.4 QL. The (ABC) stacking sequence is unchanged over the boundary. However, only three atomic sheets within a QL completely match, while two other sheets change from Bi to Te and vice versa. The steps do not vanish during island coalescence. Moreover, they maintain undisturbed, while overgrown by next QLs in the step-flow mode and, hence, propagate throughout the entire film. The presence of the domains is independent of the surface preparation and, therefore, is not defined by the nucleation and growth dynamics. The study will help to understand properties of the MBE growth and substrate influence on complex TI material systems in order to improve their structural and electrical properties.

¹D. Hsieh, Y. Xia, D. Qian, L. Wray, J. H. Dil, F. Meier, J. Osterwalder, L. Patthey, J. G. Checkelsky, N. P. Ong, A. V. Fedorov, H. Lin, A. Bansil, D.

- Grauer, Y. S. Hor, R. J. Cava, and M. Z. Hasan, *Nature (London)* **460**, 1101 (2009).
- ²M. Z. Hasan and C. L. Kane, *Rev. Mod. Phys.* **82**, 3045 (2010).
- ³Y.-Y. Li, G. Wang, X.-G. Zhu, M.-H. Liu, C. Ye, X. Chen, Y.-Y. Wang, K. He, L.-L. Wang, X.-C. Ma, H.-J. Zhang, X. Dai, Z. Fang, X.-C. Xie, Y. Liu, X.-L. Qi, J.-F. Jia, S.-C. Zhang, and Q.-K. Xue, *Adv. Mater.* **22**, 4002 (2010).
- ⁴L. Plucinski, G. Mussler, J. Krumrain, A. Herdt, S. Suga, D. Grützmacher, and C. M. Schneider, *Appl. Phys. Lett.* **98**, 222503 (2011).
- ⁵J. Horák, J. K. Čermák, and L. Koudelka, *J. Phys. Chem. Solids* **47**, 805 (1986).
- ⁶L. He, X. Kou, and K. L. Wang, *Phys. Status Solidi (RRL)* **7**, 50 (2013).
- ⁷W. Dang, H. Peng, H. Li, P. Wang, and Z. Liu, *Nano Lett.* **10**, 2870 (2010).
- ⁸J. Krumrain, G. Mussler, S. Borisova, T. Stoica, L. Plucinski, C. Schneider, and D. Grützmacher, *J. Cryst. Growth* **324**, 115 (2011).
- ⁹H. W. Liu, H. T. Yuan, N. Fukui, L. Zhang, J. F. Jia, Y. Iwasa, M. W. Chen, T. Hashizume, T. Sakurai, and Q. K. Xue, *Cryst. Growth Des.* **10**, 4491 (2010).
- ¹⁰X. Liua, D. J. Smith, H. Cao, Y. P. Chen, J. Fan, and Y.-H. Zhang, *J. Vac. Sci. Technol. B* **30**, 02B103 (2012).
- ¹¹N. V. Tarakina, S. Schreyeck, T. Borzenko, C. Schumacher, G. Karczewski, K. Brunner, C. Gould, H. Buhmann, and L. W. Molenkamp, *Cryst. Growth Des.* **12**, 1913 (2012).
- ¹²A. Koma, *Surf. Sci.* **267**, 29 (1992).
- ¹³A. Koma, *Thin Solid Films* **216**, 72 (1992).
- ¹⁴H. Kawanami, A. Hatayama, and Y. Hayashi, *J. Electron. Mater.* **17**, 341 (1988).
- ¹⁵M. Kawabe and T. Ueda, *Jpn. J. Appl. Phys. Part 2* **26**, L944 (1987).
- ¹⁶N.-H. Cho and C. B. Carter, *J. Mater. Sci.* **36**, 4209–4222 (2001).
- ¹⁷S. Borisova, J. Krumrain, M. Luysberg, G. Mussler, and D. Grützmacher, *Cryst. Growth Des.* **12**, 6098 (2012).
- ¹⁸X. F. Kou, L. He, F. X. Xiu, M. R. Lang, Z. M. Liao, Y. Wang, A. V. Fedorov, X. X. Yu, J. S. Tang, G. Huang, X. W. Jiang, J. F. Zhu, J. Zou, and K. L. Wang, *Appl. Phys. Lett.* **98**, 242102 (2011).
- ¹⁹L. He, F. Xiu, Y. Wang, A. V. Fedorov, G. Huang, X. Kou, M. Lang, W. P. Beyermann, J. Zou, and K. L. Wang, *J. Appl. Phys.* **109**, 103702 (2011).
- ²⁰D. L. Medlin, Q. M. Ramasse, C. D. Spataru, and N. Y. C. Yang, *J. Appl. Phys.* **108**, 043517 (2010).
- ²¹D. L. Medlin and N. Y. C. Yang, *J. Electron. Mater.* **41**, 1456 (2012).
- ²²G. Zhang, H. Qin, J. Teng, J. Guo, Q. Guo, X. Dai, Z. Fang, and K. Wu, *Appl. Phys. Lett.* **95**, 053114 (2009).
- ²³R. W. G. Wyckoff, *Crystal Structures*, 2nd ed. (John Wiley and Sons, New York, 1964).